Available online at www.sciencedirect.com

ScienceDirect

IFAC Papers Online CONFERENCE PAPER ARCHIVE

IFAC PapersOnLine 50-1 (2017) 6320–6325

Time-Optimal Solution for a Unicycle Path on SE(2) with a Penalty on Curvature ⋆

Udit Halder * **Uroš Kalabić** **

* *Department of Electrical and Computer Engineering, University of Maryland, College Park, MD 20742 USA (e-mail: udit@umd.edu)*
** *Mitsubishi Electric Research Laboratories, Cambridge, MA 02139 USA (e-mail: kalabic@merl.com)*

Abstract: This work considers the problem of minimizing the path-curvature of a unicycle moving between two configurations in SE(2) with free final time. The problem is posed as an optimal control problem and the necessary conditions are derived using the Pontryagin Maximum Principle and Lie-Poisson reduction. Solutions are categorized into three cases corresponding to the value of the Casimir. A numerical solver for obtaining the optimal control is described. Experimental results are reported on a ground robot.

Keywords: Path planning; Optimal trajectory; Optimal control; Geometric approaches; Continuous path control; Time-optimal control

1. INTRODUCTION

The kinematic unicycle model is often used in path-planning for ground vehicles, since the configuration of a ground vehicle can often be represented by a point in a plane that is constrained to move in the direction of the current heading (Bellaïche et al., 1998). The state of this system can be represented as an element of the special Euclidean group SE(2), where the control inputs are a curvature input which controls the rate of change of the heading angle, and a velocity input which controls the rate of change of the unicycle position in the direction of the heading angle.

Given the current configuration of the unicycle and a desired future configuration, an admissible path for moving the unicycle from an initial to a final configuration can be determined via the minimization of some cost functional. Particularly elegant and well-known examples of a solution to such an optimization are the minimum-time solutions of Dubins (1957) and Reeds and Shepp (1990). Optimal paths of the minimum-time problem consist only of straight-line and circular-arc segments which, when patched together, create discontinuities in the path curvature and cause potential difficulty in implementation since abrupt changes in curvature are hard to track. Proposed modifications that alleviate this problem enforce that the curvature stay continuous, *e.g.*, Fraichard and Scheuer (2004), yet it is also possible to penalize the total curvature along the path in the expectation that the optimal curvature will be continuous. In this paper, we take the latter approach, considering the minimization of the curvature along a path connecting initial and final unicycle configurations with free final time.

Our solution is obtained using geometric optimal control, where the necessary conditions for optimality are obtained via the Pontryagin Maximum Principle (PMP), and Lie-Poisson reduction (Krishnaprasad, 1993; Ohsawa, 2013). Using geometric optimal control on SE(2) to find solutions to path-planning problems has also been considered by Sussmann and Tang (1991) and Agrachev and Sachkov (2004). The difference between our work and that of Krishnaprasad (1993), Dey and Krishnaprasad (2014), and Justh and Krishnaprasad (2015) is that these authors have considered a different kind of penalty.

As mentioned, the solution to the minimum-curvature problem is obtained using optimal control. From the necessary conditions, we show that there are two constants of motion: the Hamiltonian, which is zero due to time-optimality, and the Casimir. We show that there are three possible families of solutions depending on the Casimir. In the first case, the motion consists of segments of a U-turn; in the second case, the motion consists of straight lines or asymptotic approaches thereto; in the third case, the motion consists of segments of parallel parking trajectories. After the cases have been enumerated, we provide a numerical solver that obtains the solution to the optimal control problem. In the last part of the paper, we present experimental results on a ground robot, whose dynamics are that of a unicycle. The results show good tracking of the curvature and velocity inputs.

The paper is organized as follows. In Section 2, we introduce the problem. In Section 3 we derive the solution, enumerate the possible cases, and present a numerical solver. In Section 4, we present experimental results. Section 5 is the conclusion.

2. PROBLEM FORMULATION

In this work, we consider minimizing the curvature of a path in $\mathbb{R}^2$ connecting an initial unicycle configuration g_i with its desired final configuration g_f. Since unicycle configurations can be represented as elements of SE(2), we

⋆ This work was sponsored by the Mitsubishi Electric Research Laboratories.

10.1016/j.ifacol.2017.08.916

formulate this optimization as a geometric optimal control problem and derive the necessary conditions using PMP and Lie-Poisson reduction.

Consider the unicycle kinematic equations,

$$\dot{x}(t) = v(t)\cos\theta(t), \tag{1a}$$
$$\dot{y}(t) = v(t)\sin\theta(t), \tag{1b}$$
$$\dot{\theta}(t) = u(t), \tag{1c}$$

where $(x(t), y(t)) \in \mathbb{R}^2$ is the position of the unicycle on the Cartesian plane, $\theta(t) \in \mathbb{R}$ is the heading of the unicycle, $v(t)$ is the unicycle velocity, which is constrained between ± 1, and $u(t)$ is the signed path curvature, equal to the rate of change of the heading $\theta(t)$.

The configuration of the unicycle can be represented as an element of the matrix Lie group SE(2). Let $g(t) \in \mathrm{SE}(2)$ where,

$$g(t) = \begin{bmatrix} \cos\theta(t) & -\sin\theta(t) & x(t) \\ \sin\theta(t) & \cos\theta(t) & y(t) \\ 0 & 0 & 1 \end{bmatrix}. \tag{2}$$

Then the equations (1) can be written in left-invariant form,

$$\dot{g}(t) = g(t)\xi(u(t), v(t)), \tag{3}$$

where,

$$\xi(u(t), v(t)) = u(t)X_1 + v(t)X_2, \tag{4}$$

and,

$$X_1 = \begin{bmatrix} 0 & -1 & 0 \\ 1 & 0 & 0 \\ 0 & 0 & 0 \end{bmatrix}, \; X_2 = \begin{bmatrix} 0 & 0 & 1 \\ 0 & 0 & 0 \\ 0 & 0 & 0 \end{bmatrix}. \tag{5}$$

The matrices X_1 and X_2 are elements of the Lie algebra $\mathfrak{se}(2)$. Together with $X_3 = [X_1, X_2] = X_1X_2 - X_2X_1$, X_1 and X_2 form a basis for $\mathfrak{se}(2)$.

Without loss of generality, we can assume that $g_0 = I_3$, since $g(t)$ can always be redefined according to $g(t) := g_0^{-1}g(t)$. The final time t_f is free and the cost function to be minimized is,

$$\frac{1}{2}\int_0^{t_f} \left(1 + au(t)^2\right) dt, \tag{6}$$

where $a > 0$ is a scalar penalty. Note that the problem is not well-posed without a penalty on time, since otherwise a solution does not necessarily exist. Without a penalty on time, unless $u(t) \equiv 0$, the final time may be infinite.

3. OPTIMAL CONTROL SOLUTION

In order to solve the problem we form the pre-Hamiltonian,

$$H = \langle p, g\xi(u, v)\rangle - \frac{1}{2}(1 + au^2), \tag{7}$$

where $p(t) \in \mathrm{SE}(2)^*$ is the adjoint variable. To simplify the Hamiltonian, we perform Lie-Poisson reduction, introducing the variable $\mu(t) \in \mathfrak{se}(2)^*$ satisfying the translation to identity,

$$\langle \mu, \xi(u, v)\rangle = \langle p, g\xi(u, v)\rangle.$$

As an element of the dual space, $\mu(t)$ can be represented as $\mu(t) = \mu_1 X_1^\flat + \mu_2 X_2^\flat + \mu_3 X_3^\flat$, where $\{X_1^\flat, X_2^\flat, X_3^\flat\}$ are the basis vectors dual to $\{X_1, X_2, X_3\}$.

The pre-Hamiltonian therefore becomes,

$$\begin{aligned} H(\mu, u, v) &= \langle \mu, \xi(u, v)\rangle - \frac{1}{2}(1 + au^2), \\ &= \langle \mu_1 X_1^\flat + \mu_2 X_2^\flat + \mu_3 X_3^\flat, uX_1 + vX_2\rangle \\ &\qquad - \frac{1}{2}(1 + au^2), \\ &= \mu_1 u + \mu_2 v - \frac{1}{2}(1 + au^2). \end{aligned}$$

According to PMP, the optimal control (u^*, v^*) satisfies,

$$H(\mu^*, u^*, v^*) = \max_{u\in\mathbb{R},\; v\in[-1,1]} H(\mu^*, u, v). \tag{8}$$

Therefore the optimal controls are given by,

$$u^* = \mu_1/a, \tag{9}$$
$$v^* = \operatorname{sgn}\mu_2, \;\; \mu_2 \neq 0, \tag{10}$$

where sgn is the signum function and $v^* \in [-1, 1]$ can take any value when $\mu_2 = 0$. The reduced Hamiltonian is therefore,

$$h = H(\mu, u^*, v^*) = \frac{1}{2}\mu_1^2/a + |\mu_2| - \frac{1}{2}, \tag{11}$$

and the dynamics of the μ_i variables are given by (Krishnaprasad, 1993),

$$\begin{bmatrix} \dot{\mu}_1 \\ \dot{\mu}_2 \\ \dot{\mu}_3 \end{bmatrix} = \begin{bmatrix} 0 & -\mu_3 & \mu_2 \\ \mu_3 & 0 & 0 \\ -\mu_2 & 0 & 0 \end{bmatrix} \frac{\partial h}{\partial(\mu_1, \mu_2, \mu_3)}, \tag{12}$$

$$\dot{\mu}_1 = -\mu_3 \operatorname{sgn}\mu_2, \tag{13a}$$
$$\dot{\mu}_2 = \mu_1\mu_3/a, \tag{13b}$$
$$\dot{\mu}_3 = -\mu_1\mu_2/a. \tag{13c}$$

Let,

$$c = \mu_2^2 + \mu_3^2. \tag{14}$$

This variable is called the Casimir and it is a constant of motion, implying that the variables μ_2 and μ_3 evolve on circle of radius $\sqrt{c}$. Along with the Casimir, the Hamiltonian (11) is also a conserved quantity of motion. Since the final time is free, the Hamiltonian must be equal to 0, resulting in the constraint,

$$|\mu_2| = \frac{1}{2}(1 - \mu_1^2/a). \tag{15}$$

Note that, according to the above constraint, the curvature u is constrained between $\pm 1/\sqrt{a}$. This is an interesting and useful fact, since it can be used in the control design. For example, if it is known that $u_{\max}$ is the maximum allowable heading rate of change $\dot{\theta}$, or equivalently the maximum allowable curvature u, then a natural choice of penalty would be to set $a \geq 1/u_{\max}^2$.

3.1 Characterizing the Types of Motion

According to (14) and (15), the dynamics (13) evolve on the manifold $\mathcal{M}_c$ where,

$$\begin{aligned} \mathcal{M}_c &= \mathcal{C}_c \cap \mathcal{H}, \\ \mathcal{C}_c &= \{(\mu_1, \mu_2, \mu_3) \in \mathbb{R}^3 : c = \mu_2^2 + \mu_3^2)\}, \\ \mathcal{H} &= \{(\mu_1, \mu_2, \mu_3) \in \mathbb{R}^3 : |\mu_2| = \frac{1}{2}(1 - \mu_1^2/a)\}. \end{aligned}$$

The manifold $\mathcal{M}_c$ is one-dimensional and equal to the intersection of a cylinder given by $\mathcal{C}_c$ and the cylinder-like shape $\mathcal{H}$. The shape of $\mathcal{M}_c$ is determined by the Casimir c. The constraint (15) is fixed, and therefore the shape of $\mathcal{H}$

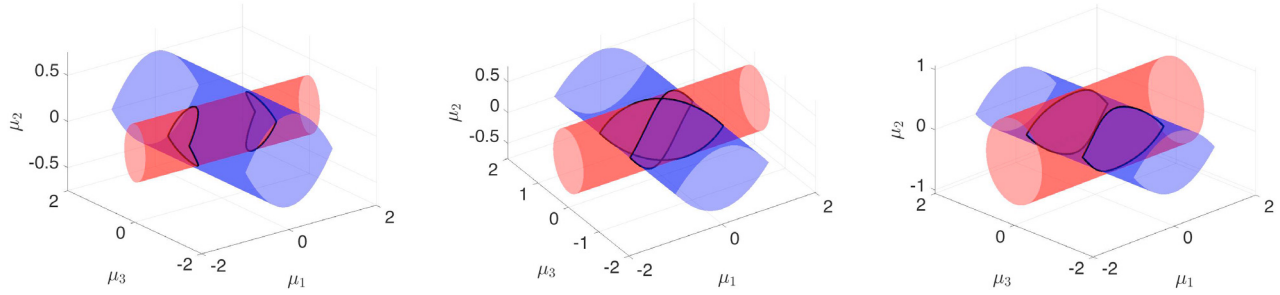

(a) $c = 0.1$ (b) $c = \frac{1}{4}$ (c) $c = 0.5$

Fig. 1. $\mathcal{M}_c$ (black) plotted as an intersection of $\mathcal{C}_c$ (red) and $\mathcal{H}$ (blue) for $a = 1$ and three values of the Casimir c

does not change with c. On the other hand, $\sqrt{c}$ is equal to the radius of the cylinder $\mathcal{C}_c$. The smallest possible cylinder $\mathcal{C}_0$ is really a line and, since there exists no upper bound on c, $\mathcal{C}_c$ can have an arbitrarily large radius.

The motion of μ evolves on $\mathcal{M}_c$. Due to continuity, it must evolve on a connected component of $\mathcal{M}_c$, so it is important to consider the types of possible intersections, of which there are three corresponding to three different cases: in Case 1, $\mathcal{C}_c$ is strictly smaller than $\mathcal{H}$; in Case 2, $\mathcal{C}_c$ is equal in size to $\mathcal{H}$; in Case 3, $\mathcal{C}_c$ is strictly larger than $\mathcal{H}$. To perform a case-by-case categorization $\mathcal{M}_c$, we note that, according to (14), the variable μ_2 is restricted to $\pm\sqrt{c}$ and, according to (15), μ_2 is restricted to $\pm\frac{1}{2}$. In Case 1, $c < \frac{1}{4}$, so $|\mu_2| \leq \sqrt{c} < \frac{1}{2}$. Therefore the motion evolves on a connected component of $\mathcal{M}_c$ where μ_1 does not change sign since $\mu_1^2 = a - 2a|\mu_2| \geq a - 2a\sqrt{c} > 0$. In Case 2, $c = \frac{1}{4}$, so the two constraints agree at the extremes and $\mathcal{M}_c$ consists of one connected component. In Case 3, $c > \frac{1}{4}$, so $|\mu_2| \leq \frac{1}{2} < \sqrt{c}$. The motion evolves on a connected component of $\mathcal{M}_c$ where μ_3 does not change sign since $\mu_3^2 = c - \mu_2^2 \geq c - \frac{1}{4} > 0$. See Fig. 1 for a visualization of the three cases. In the following, we study the three types of motion in further detail.

3.2 Change of Variables

We now follow the procedure (Jurdjevic, 1997), in which the independent variable is changed from t to θ in order to simplify the problem and obtain a solution. Note that $\mu_1/a = u = \dot{\theta}$. Therefore the solution to (13b)-(13c) is,

$$\mu_2 = \sqrt{c}\sin(\theta + \theta_0), \tag{16a}$$

$$\mu_3 = \sqrt{c}\cos(\theta + \theta_0), \tag{16b}$$

for some constant θ_0. According to (15),

$$\mu_1 = \pm\sqrt{a}\sqrt{1 - 2\sqrt{c}|\sin(\theta + \theta_0)|}. \tag{17}$$

According to the chain rule,

$$\frac{dx}{dt} = \frac{dx}{d\theta}\frac{d\theta}{dt}, \quad \frac{dy}{dt} = \frac{dy}{d\theta}\frac{d\theta}{dt}.$$

Note that $v = \operatorname{sgn}\mu_2 = \operatorname{sgn}(\sin(\theta + \theta_0))$ and,

$$\dot{\theta} = \pm\sqrt{1 - 2\sqrt{c}|\sin(\theta + \theta_0)|}\Big/\sqrt{a}. \tag{18}$$

Solving for $\frac{dx}{d\theta}$ and $\frac{dy}{d\theta}$, we obtain,

$$\frac{dx}{d\theta} = \frac{\dot{x}}{\dot{\theta}} = f^{\pm}_{c,\theta_0}(\theta)\cos\theta, \quad \frac{dy}{d\theta} = \frac{\dot{y}}{\dot{\theta}} = f^{\pm}_{c,\theta_0}(\theta)\sin\theta. \tag{19}$$

where,

$$f^{\pm}_{c,\theta_0}(\theta) = \frac{\sqrt{a}\operatorname{sgn}(\sin(\theta + \theta_0))}{\pm\sqrt{1 - 2\sqrt{c}|\sin(\theta + \theta_0)|}}, \tag{20}$$

has been introduced in order to simplify subsequent exposition.

We proceed case by case, using the expressions (19) and the initial conditions $(x(0), y(0), \theta(0)) = (0, 0, 0)$ in order to obtain a solution in the variable θ. For the subsequent analysis, we set $a = 1$.

3.3 Case 1: $c < \frac{1}{4}$

In the first case, we consider the situation when $c < \frac{1}{4}$. Here, since μ_1 does not change sign, θ is monotonic and therefore we can parametrize the solution by θ.

Proposition 1. Assume $c < \frac{1}{4}$. Let,

$$\gamma_c(\theta) = \int_0^{\theta} f^{+}_{c,0}(\theta')\begin{bmatrix}\cos\theta' \\ \sin\theta'\end{bmatrix} d\theta'. \tag{21}$$

Then,

$$\begin{bmatrix}x(t) \\ y(t)\end{bmatrix} = C(\theta_0, \pm)^{\mathrm{T}}(\gamma_c(\theta(t) + \theta_0) - \gamma_c(\theta_0)), \tag{22}$$

for some $\theta_0 \in [0, 2\pi)$, where $C(\theta_0, \pm)$ is the orthogonal matrix,

$$C(\theta_0, \pm) = \pm\begin{bmatrix}\cos\theta_0 & -\sin\theta_0 \\ \sin\theta_0 & \cos\theta_0\end{bmatrix}.$$

Proof. Since $c < \frac{1}{4}$, μ_1 and therefore $\dot{\theta}(t)$ do not change sign. Therefore, we integrate (19) to obtain the solution,

$$\begin{bmatrix}x(t) \\ y(t)\end{bmatrix} = \int_0^{\theta(t)} f^{\pm}_{c,\theta_0}(\theta')\begin{bmatrix}\cos(\theta') \\ \sin(\theta')\end{bmatrix} d\theta'$$

Performing a change of integration variables, we obtain the equivalent expression,

$$\begin{bmatrix}x(t) \\ y(t)\end{bmatrix} = \int_{\theta_0}^{\theta(t)+\theta_0} \pm f^{+}_{c,0}(\theta')\begin{bmatrix}\cos(\theta' - \theta_0) \\ \sin(\theta' - \theta_0)\end{bmatrix} d\theta'.$$

Since,

$$\begin{bmatrix}\cos(\theta' - \theta_0) \\ \sin(\theta' - \theta_0)\end{bmatrix} = C(\theta_0, +)^{\mathrm{T}}\begin{bmatrix}\cos(\theta') \\ \sin(\theta')\end{bmatrix}, \tag{23}$$

and $\int_{\theta_0}^{\theta(t)+\theta_0} = \int_0^{\theta(t)+\theta_0} - \int_0^{\theta_0}$, the result (22) follows.

Since the expression in (22) is periodic in θ_0 with period 2π, any solution implies the existence of the same solution with $0 \leq \theta_0 < 2\pi$. □

Discussion: Note that $(x(0), y(0), \theta(0)) = (0, 0, 0)$ satisfies the initial conditions. To ensure that the final conditions are satisfied, we can vary three parameters: c, θ_0, and $\pm$.

Four solution trajectories are shown in Fig. 2a. The curve γ_c corresponds to a solution where $\theta_0 = 0$ and $\mu_1 > 0$. In Fig. 2a, we show that increasing c corresponds to "stretching" the solution curve; changing θ_0 corresponds to choosing a point on γ_c and centering the curve at $\gamma_c(\theta_0)$, simultaneously rotating the curve about the origin so that the tangent vector at the origin has a heading of 0; changing the sign of $\pm$ corresponds to rotating the curve about the origin by π.

3.4 Case 2: $c = \frac{1}{4}$

The second case is transitional between the case where $c < \frac{1}{4}$ and the case where $c > \frac{1}{4}$. The manifold $\mathcal{M}_{\frac{1}{4}}$ consists of one connected component, but the motion can only occur on a particular branch. To see this, consider the situation where $-\pi/2 < \theta_0 < \pi/2$. When $c = \frac{1}{4}$, $\int_0^{\pi/2-\theta_0} \frac{d\theta}{\pm\sqrt{1-2\sqrt{c}|\sin(\theta+\theta_0)|}} = \int_0^{\pi/2-\theta_0} \frac{d\theta}{\pm\sqrt{1-|\sin(\theta+\theta_0)|}} = \pm\infty$, and therefore the time taken for θ to go from 0 to $\pi/2 - \theta_0$ is infinite.

Proposition 2. Assume $c = \frac{1}{4}$. Let,

$$\gamma_{\frac{1}{4}}(\theta) = \int_0^{\theta} f^{+}_{\frac{1}{4},0}(\theta') \begin{bmatrix} \cos\theta' \\ \sin\theta' \end{bmatrix} d\theta'. \tag{24}$$

If $\theta_0 = \frac{1}{2}\pi + n\pi$ for some integer n, $(x(t), y(t)) = (\pm t, 0)$. Otherwise,

$$\begin{bmatrix} x(t) \\ y(t) \end{bmatrix} = C(\theta_0, \pm)^{\mathrm{T}}(\gamma_{\frac{1}{4}}(\theta(t) + \theta_0) - \gamma_{\frac{1}{4}}(\theta_0)), \tag{25}$$

and $\theta_0 \in (-\pi/2, \pi/2)$.

Proof. If $\theta_0 = \frac{1}{2}\pi + n\pi$, $\dot\theta = 0$. Therefore $\theta(t) = 0$ is constant for all $t \geq 0$. Furthermore $\dot x(t) = \pm\cos(\theta(t)) = \pm 1$ and $\dot y(t) = \pm\sin(\theta(t)) = 0$ imply that $x(t) = \pm t$ and $y(t) = 0$. The rest of the proof is similar to the proof of Proposition 1.

Discussion: This case consists of two types of solutions: a straight line solution, corresponding to the subcase where the final condition lies on the x-axis, and an asymptotic solution, which asymptotically approaches a straight line with slope $\cot\theta_0$.

As in the previous case, varying the parameter θ_0 corresponds to a rotation of the solution curve and changing the sign of $\pm$ corresponds to a rotation of the curve by π. Note that, due to the definition of (24), the value of θ_0 is restricted to between $\pm\pi/2$ because the solution goes to infinity at $\theta = \pm\pi/2 - \theta_0$. See Fig. 2b for a graphic.

3.5 Case 3: $c > \frac{1}{4}$

In the third case, we consider the situation when $c > \frac{1}{4}$. Here, θ is periodic unlike in the previous two cases. This is proved in the following result.

Lemma 3. Assume $c > \frac{1}{4}$. Let θ_c be the solution to,

$$\sin\theta_c = \frac{1}{2\sqrt{c}} < 1,\ 0 < \theta_c < \pi/2. \tag{26}$$

Let $\vartheta'(t)$ be the solution to,

$$\dot\vartheta' = \sqrt{1 - 2\sqrt{c}|\sin\vartheta'|},$$

with initial condition $\vartheta'(0) = 0$. The solution exists and is real over the time interval $[-t_c, t_c]$, where $\vartheta'(-t_c) = -\theta_c$ and $\vartheta'(t_c) = \theta_c$. Define,

$$\vartheta(t) = \vartheta'(t - 2nt_c) + 2n\theta_c,\ n = \lfloor t/2t_c \rceil, \tag{27}$$

and let $\theta(\vartheta) = (-1)^n(\vartheta - 2n\theta_c),\ n = \lfloor \vartheta/2\theta_c \rceil$. Assume $\theta(0) = 0$. Then $\theta(t) = \theta(\vartheta(t))$.

Proof. The time $t_c > 0$ exists and is finite because $0 < \theta_c < \pi/2$ and $t_c = \frac{1}{2}\int_{-\theta_c}^{\theta_c} \frac{d\vartheta'}{\sqrt{1-2\sqrt{c}|\sin\vartheta'|}} < \infty$. Due to the definition of θ_c, the expression under the square root is non-negative for all $-\theta_c \leq \vartheta' \leq \theta_c$, implying that $\vartheta_c(t)$ exists and is real over $[-t_c, t_c]$.

Whenever $\theta = \pm\theta_c$, $|\dot\mu_1| = |-\mu_3 \operatorname{sgn}\mu_2| > 0$. Therefore, $(x(\pm\theta_c), y(\pm\theta_c))$ are not equilibrium points. Since the solution must stay in a connected component of $\mathcal{M}_c$, this implies that $\dot\theta$ changes sign whenever $\theta = \pm\theta_c$.

Due to the reversal of sign, $\theta(t) = -(\vartheta'(t - 2t_c) - 2\theta_c) = -(\vartheta(t) - 2\theta_c)$ for $t \in [t_c, 3t_c]$. The sign changes with period $2t_c$. Therefore, due to symmetry, $\theta(t)$ is periodic with period $4t_c$. The previous two statements imply that $\theta(t) = \theta(\vartheta(t))$ when $\theta(0) = 0$. □

Because of the periodicity of θ, we have introduced the monotonic variable ϑ, to parametrize the solution curve.

Proposition 4. Assume $c > \frac{1}{4}$. Let,

$$\gamma_c(\vartheta) = \int_0^{\vartheta} f^{+}_{c,0}(\theta(\hat\vartheta)) \begin{bmatrix} \cos(\theta(\hat\vartheta)) \\ \sin(\theta(\hat\vartheta)) \end{bmatrix} d\hat\vartheta. \tag{28}$$

Then,

$$\begin{bmatrix} x(t) \\ y(t) \end{bmatrix} = C(\vartheta_0, \pm)^{\mathrm{T}}(\gamma_c(\vartheta(t) + \vartheta_0) - \gamma_c(\vartheta_0)), \tag{29}$$

where $\vartheta_0 \in [0, 4\theta_c)$.

Discussion: Similar to Case 1, varying the parameter c results in changing the shape of the curve, where increasing c "compresses" the curve; increasing the parameter θ_0 corresponds to a translation and rotation of the γ_c; and changing the sign of $\pm$ corresponds to a rotation of the curve by π. See Fig. 2c for a graphical representation.

3.6 Numerical Solver

Given a desired final configuration, we must consider every possible case that satisfies the necessary conditions. In the following, we describe our case-by-case numerical solution to the optimal control problem.

Case 1: We solve (22) for $c \in [0, 1/4)$ and $\theta_0 \in [0, 2\pi)$ numerically. We have obtained a result outside the scope of this work that $\theta(t_f)$ must be within $\pm\pi$. This limits our search to two possible solutions, corresponding to the possible values of $\operatorname{sgn}\mu_1(0)$. For the initial condition, we set $\theta_0 = 0$ and c to be the solution of $\|\gamma_c(\pi)\| = \|(x_f, y_f)\|$.

Case 2: If possible, we connect the initial and final conditions by a line segment. If not, we attempt to solve (25) for $\theta_0 \in (-\pi/2, \pi/2)$, for two possible values of $\operatorname{sgn}\mu_1(0)$.

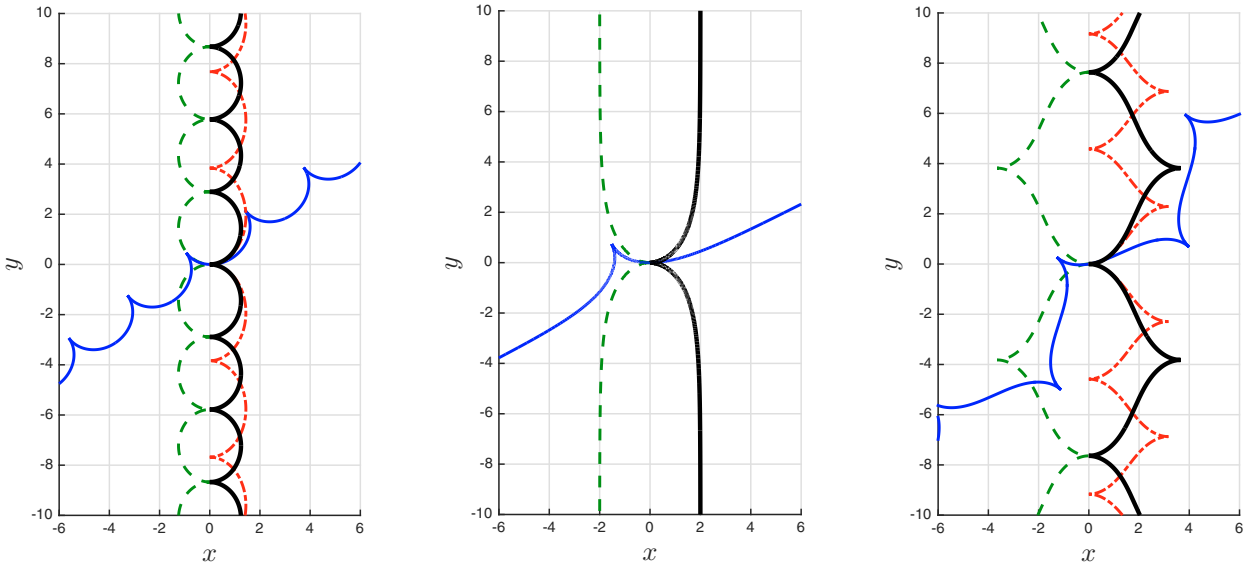

(a) $c = 0.1$ (solid black) and 0.18 (dot-dashed red)

(b) $c = \frac{1}{4}$

(c) $c = 0.3$ (solid black) and 0.4 (dot-dashed red)

Fig. 2. γ_c for different cases (solid black) – increasing c produces the dot-dashed red curve; increasing θ_0 produces the solid blue curve; changing the sign from + to − produces the dashed green curve

Case 3: We solve (29) for $c > 1/4$ and $\vartheta_0 \in [0, 4\theta_c)$. We have obtained a result outside the scope of this work that $\vartheta(t_f)$ must be within $\pm 4\theta_c$. Since θ is periodic in ϑ, it can assume the value θ_f twice in $[0, 4\theta_c]$. Hence, for each value of $\operatorname{sgn}\mu_1(0)$, we solve for an additional subcase, bringing the total number of subcases considered to four. For the initial condition, we set $\theta_0 = 0$ and c to be the solution of $\|\gamma_c(4\theta_c)\| = \|(x_f, y_f)\|$.

For each case, if the solver times out or becomes unstable, we terminate the process as a solution to the problem likely does not exist. After computing all possibilities that satisfy the necessary conditions, we compare each and choose the one with minimum cost.

4. EXPERIMENTAL RESULTS

We provide a laboratory demonstration using a mobile ground robot. The test platform consists of a Pioneer P3-DX differential drive robot which has width of 380 mm and a swing radius of 260 mm. The robot is equipped with reversible DC motors and high resolution motion encoders. The control station is a computer running ROS (Robot Operating System), which wirelessly sends commands to the robot. We use ROS-ARIA as an interface for controlling the robot. A Vicon motion capture system is used to track the robot trajectory and the control commands are sent to the robot via the MATLAB ROS toolbox.

We design a feedback controller to track the optimal trajectory. Given the optimal reference trajectory (x_r, y_r, θ_r) and optimal reference control inputs (u_r, v_r), we use the trajectory tracking scheme from Kanayama et al. (1990). Specifically, we define error variables,

$$\begin{bmatrix} x_e \\ y_e \\ \theta_e \end{bmatrix} = \begin{bmatrix} \cos\theta & \sin\theta & 0 \\ -\sin\theta & \cos\theta & 0 \\ 0 & 0 & 1 \end{bmatrix} \begin{bmatrix} x_r - x \\ y_r - y \\ \theta_r - \theta \end{bmatrix}, \tag{30}$$

so that the error dynamics are given by,

$$\begin{bmatrix} \dot{x}_e \\ \dot{y}_e \\ \dot{\theta}_e \end{bmatrix} = \begin{bmatrix} u y_e - v + v_r \cos\theta_e \\ -u x_e + v_r \sin\theta_e \\ u_r - u \end{bmatrix}, \tag{31}$$

where (x, y, θ) is the system state and (u, v) are the control inputs. As proposed by Panteley et al. (1998), we choose our stabilizing controls to be,

$$u = u_r + c_1\theta_e \tag{32a}$$

$$v = v_r + c_2 x_e, \tag{32b}$$

for some parameters $c_1, c_2 > 0$.

The experimental results of two trials are presented in Figs. 3-4 corresponding to two different final conditions. The parameters for both trials were set to $a = 1$, $|v_r| = 0.2$m/s, $c_1 = 2$Hz, and $c_2 = 0.5$Hz. The robot trajectory (x, y, θ) is presented in Fig. 3 along with the associated optimal trajectory (x_r, y_r, θ_r). The inputs (u_r, v_r) and (u, v) are plotted in Fig. 4. The 2-norms of the final position errors are 62.8mm and 124.5mm for the first and second trial, respectively. Both errors are on the order of the size of the robot, which has a radius of 260mm. The final heading errors are 3.02° and 4.74°, respectively.

5. CONCLUSION

In this paper, we considered the problem of determining the minimum-curvature path of a unicycle between two configurations in SE(2). Techniques from geometric optimal control were used in order to obtain the necessary conditions in Lie-Poisson reduced variables. Three possible types of paths were presented, which depend on the value of the Casimir. Experimental results were presented, which showed a ground robot tracking the optimal path.

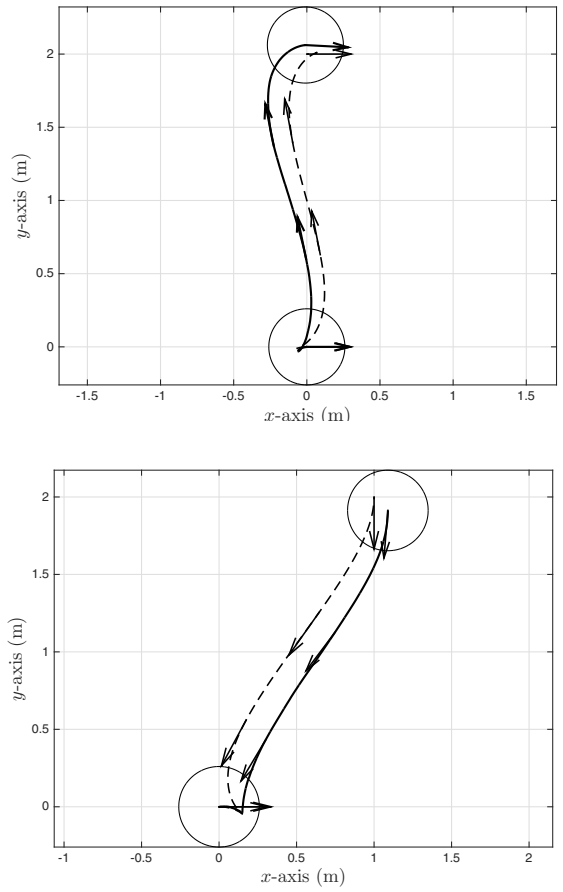

Fig. 3. Experimental results with robot trajectories (solid), associated optimal paths (dashed), headings (arrows), and initial positions, both $(0, 0, 0)$, and final positions, $(0\text{m}, 2\text{m}, 0)$ and $(1\text{m}, 2\text{m}, -\frac{\pi}{2})$, of the ground robot (circles)

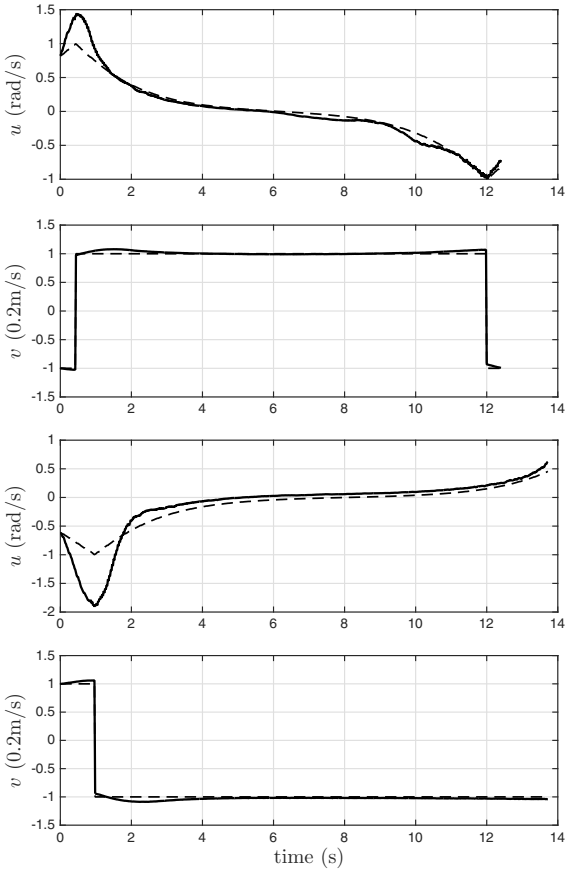

Fig. 4. Plots of $(u_r(t), v_r(t))$ (dashed) and $(u(t), v(t))$ (solid)

ACKNOWLEDGEMENTS

The authors acknowledge Dr. Rohit Gupta of the University of Minnesota and Dr. Stefano Di Cairano and Dr. Yebin Wang of the Mitsubishi Electric Research Laboratories for technical discussions, and Prof. P.S. Krishnaprasad of the University of Maryland for allowing the use of laboratory space and experimental equipment.

REFERENCES

Agrachev, A. and Sachkov, Y. (2004). *Control Theory from the Geometric Viewpoint*. Springer, Berlin.

Bellaïche, A., Jean, F., and Risler, J.J. (1998). Geometry of nonholonomic systems. In J.P. Laumond (ed.), *Robot Motion Planning and Control*. Springer, London.

Dey, B. and Krishnaprasad, P.S. (2014). Control-theoretic data smoothing. In *Proc. IEEE Conf. Decision and Control*, 5064–5070. Los Angeles, CA.

Dubins, L.E. (1957). On curves of minimal length with a constraint on average curvature, and with prescribed initial and terminal positions and tangents. *American J. Math.*, 79(3), 497–516.

Fraichard, T. and Scheuer, A. (2004). From Reeds and Shepp's to continuous-curvature paths. *IEEE Trans. Robotics*, 20(5), 1025–1035.

Jurdjevic, V. (1997). *Geometric Control Theory*. Cambridge University Press, Cambridge, England.

Justh, E.W. and Krishnaprasad, P.S. (2015). Optimality, reduction and collective motion. *Proc. Roy. Soc. A*, 471(2177).

Kanayama, Y., Kimura, Y., Miyazaki, F., and Noguchi, T. (1990). A stable tracking control method for an autonomous mobile robot. In *Proc. IEEE Int. Conf. Robotics and Automation*, 384–389. Cincinnati, OH.

Krishnaprasad, P.S. (1993). Optimal control and Poisson reduction. Technical Report 93-87, Institute for Systems Research, University of Maryland.

Ohsawa, T. (2013). Symmetry reduction of optimal control systems and principal connections. *SIAM J. Control Optim.*, 51(1), 96–120.

Panteley, E., Lefeber, E., Loria, A., and Nijmeijer, H. (1998). Exponential tracking control of a mobile car using a cascaded approach. In *Proc. IFAC Workshop Motion Control*, 221–226. Grenoble, France.

Reeds, J. and Shepp, L. (1990). Optimal paths for a car that goes both forwards and backwards. *Pacific J. Math.*, 145(2), 367–393.

Sussmann, H.J. and Tang, G. (1991). Shortest paths for the Reeds-Shepp car: A worked out example of the use of geometric techniques in nonlinear optimal control. Technical Report 91-10, Rutgers Center for Systems and Control.